Research   **Open Access**

Association between Arctic Circulation and Indian Summer Monsoon Rainfall

Santosh Kakade [*] **and Ashwini Kulkarni**

Indian Institute of Tropical Meteorology, Pune, India

*Corresponding author: Santosh Kakade, Indian Institute of Tropical Meteorology, Dr. Homi Bhabha Road, Pashan Pune, India, Tel: 020 2590 4200, E-mail: kakade@tropmet.res.in

Abstract

The cluster regions for different meteorological fields at lower, mid and upper troposphere are identified using Shared Nearest Neighbor (SNN) algorithm. The relationships among weather conditions over the Arctic cluster regions, Indian Summer Monsoon Rainfall (ISMR) and Arctic oscillation are studied. It is observed that Arctic oscillation and mid tropospheric zonal wind anomaly over cluster region [60°N-70°N; 5°W-55°W] are directly correlated with each other in winter season and this relationship in turn influences ISMR. During contrasting phases of ESI (Effective Strength Index) tendency, the significant inverse relationship between zonal wind anomaly over Arctic clusters and ISMR show spatial and temporal variability. During positive (negative) ESI-tendency, lower tropospheric (upper tropospheric) temperature and pressure anomalies over respective cluster regions in Arctic have relationship with ISMR.

Introduction

Arctic is the North Polar Region which is north of Arctic circle (the imaginary circle passing through the Arctic Ocean, the Scandinavian Peninsula, North Asia, Northern America and Greenland). The Arctic oscillation (AO), also known as Northern Annular Mode (NAM) is time series associated with the most dominant mode of wintertime sea level pressure, north of 20°N and it is characterized by pressure anomalies of one sign in the Arctic with the opposite anomalies centered about 37°-45°N. Thompson and Wallace [1] have named the zonal sea saw between sea level pressures in polar and temperate latitudes as Arctic Oscillation (AO) and they have shown that AO is more strongly coupled with Eurasian temperature fluctuations than with North Atlantic Oscillation (NAO). It accounts for substantially large fraction of variance of northern hemisphere surface air temperature. The AO index is the degree to which Arctic air penetrates into middle latitudes. When the AO index is positive, surface pressure is low in the polar region which helps the middle latitude jet stream to blow strongly and consistently from west to east, thus keeping cold Arctic air locked in the polar region. When the AO index is negative, pressure in the polar region tends to be high, zonal winds are weaker. During its positive (negative) phase, Arctic geopotential height anomalies are negative (positive).

A large number of studies are available discussing possible linkages of AO with climate variations over Northern hemisphere. Wu et al. [2] have examined the linkage between phases of AO with wintertime climate over Canada and USA. They have shown that during positive phase of AO there is cold climate anomaly over northeastern and eastern Canada, Alaska and the west coast of USA, and a warm climate anomaly over the rest of the continent. It has been also shown that the east Asian winter monsoon is strong during the negative phase of AO [3-6].

Kakade and Dugam [7-9] have defined the index known as Effective Strength Index (ESI) as the combined strength of North Atlantic Oscillation (NAO) and Southern Oscillation (SO) and have shown that ESI decreases from January to April during excess monsoon years and vice versa. Thus ESI-tendency from January to April is a precursor for monsoon circulation over Indian subcontinent. Kakade and Kulkarni [10,11] have discussed the evolution of NAO and SO from winter to spring and their impact on European temperature changes during contrasting phases of ESI-tendency. The present study mainly deals with the relationships among AO, Arctic weather and ISMR on interannual scale during positive and negative ESI-tendency. The changes in extreme weather events modulated by long term changes in NAO have been discussed by Scaife et al. [12].

In this paper we have applied Shared Nearest Neighbour algorithm to get homogeneous clusters over Arctic region using various meteorological parameters at lowest, middle and upper atmospheric levels. There are many clustering algorithms available and have been used in climate science e.g. the hard clustering methods like map-to-map method [13,14], the distance-based k-means method [14-18], soft clustering methods like fuzzy c-menas method [19,20], machine learning techniques like self-organizing maps [21,22], and stochastic weather generators using time series resampling algorithms[23].

Section 2 describes the data used in the analysis and explains the method of Shared Nearest Neighbour (SNN) for cluster analysis in detail. The association between Arctic circulation and the Indian Summer Monsoon Rainfall has been described in section 3. Section 4 gives final conclusions.

Data and Methodology

Data

(a) Indian Summer Monsoon Rainfall (ISMR) rainfall data for June to September have been taken from the web site www.tropmet.res.in. The seasonal rainfall is computed by adding the rainfall from June to September. The percentage departure from long term (1871-2014) mean is referred as rainfall index in further analysis.

(b) ESI-tendency: Monthly index of NAO and SO for the period 1951-2014 have been obtained from www.cpc.ncep.noaa.gov. ESI is standardized value of difference between monthly NAO and SO index. ESI-tendency is defined as April-ESI minus January-ESI. During 1951-2014, there are 31 years (1951, 1954, 1955, 1957, 1960, 1962, 1963, 1965, 1967, 1969, 1972, 1974, 1976, 1977, 1980, 1981, 1982, 1985, 1987, 1990, 1991, 1992, 1994, 1996, 1997, 2001, 2002, 2004, 2006, 2009, 2011, 2012 and 2014) with positive ESI-tendency while 33 years (1952, 1953, 1956, 1958, 1959, 1961, 1964, 1966, 1968, 1970, 1971, 1973, 1975, 1978, 1979, 1983, 1984, 1986, 1988, 1989, 1993, 1995, 1998, 1999, 2000, 2003, 2005, 2007, 2008, 2010 and, 2013) with negative ESI-tendency.

(c) The NCEP/NCAR Reanalysis gridded 2.5o × 2.5o long/lat global surface air temperature (Kelvin), geo-potential height (meter), zonal wind (ms-1) data for all pre-monsoon months and seasons (January, February, March, April, May, Winter, Spring) at surface, 850-hPa, 500-hPa, 200-hPa for 1948-2014 have been taken from

http://www.esrl.noaa.gov/psd/data/gridded/
data.ncep.reanalysis.html. The data have been interpolated on 5o × 5o lat/long.

(d) Arctic Oscillation (AO) Monthly Arctic Oscillation (AO) data for the period 1951-2014 have been taken from http://www.cpc.ncep.noaa.gov/products/precip/CWlink/daily_ao_index/monthly.ao.index.b50.current.ascii.table.

Seasonal and annual AO is computed by averaging corresponding monthly AO as Winter (December-January-February), Spring (March-April-May), Summer (June-July-August), Autumn (September-October-November), Pre-monsoon (April-May), Monsoon (June-July-August-September) and Post-monsoon (October-November).

Shared nearest neighbor (SNN) algorithm

Ertoz et al. [24] have identified clusters of different sizes, shapes, and densities in noisy, high dimensional data. Steinbach et al. [24,25] discovered new climate indices using meteorological parameters like SST, SLP, precipitation using SNN algorithm. Boriah et al. [26] have identified ocean temperature clusters by SNN algorithm and used these clusters to predict land temperatures.

SNN algorithm: The seasonality is removed by computing anomalies. Any trend or autocorrelation is removed from time series at each grid if it exists.

The correlation coefficients (CCs) the time series of each grid point with remaining grids are computed and significant (at 1% level) CCs are retained. This matrix is known as similarity matrix.

The most import factor which adjusts the focus of the clusters is the neighborhood list size (k, here k=100). Each grid point 'i' has a neighbor list containing at most k number of grid points showing highest CC with i-th grid point.

The strength (str) of link between two points i and j is determined by formula described by Jarvis and Patrik [26].

Str(i, j) = Σ(k +1−m)×(k +1− n), where m and n are positions of SNNs in the lists of i and j.

The threshold value for total link strength at a grid point is decided by trial and error (here it is 100). The grid points showing greater link strength than threshold value are considered as core points for cluster formation.

Discussion

The Arctic Oscillation (AO) is the climatic pattern described by cyclonic winds circulating around 55°N latitude. During it's positive phase, the circulating winds are strong which confines strong cold easterlies and cold air-mass in Arctic region. On the other hand, negative phase of the AO allows southward penetrating of cold Arctic air-mass due to weak circulating winds. The correlations between ISMR and monthly/seasonal AO for 1951-2014 are computed. It is observed that AO prior to monsoon season is weakly correlated with ISMR. The positive significant relationship of AO with ISMR is observed in October (R=0.39), Summer (0.33), Autumn (0.43), Monsoon season (0.41) and Post-monsoon season (0.40). Interestingly the ISMR seems to have strong, statistically significant relationship with succeeding AO in Autumn season. Figure 1 shows 30 year sliding CCs of ISMR with AO in monsoon (top panel) and AO in Autumn season (bottom panel) for the period 1951-2014. It suggests the stability in the relationship ISMR and AO. The positive correlation between AO and ISMR can be interpreted as: when AO is positive then the southward penetration of Arctic cold air-mass is restricted, which may result in reducing Eurasian snow-cover and more rainfall over India [20,27,28]. AO is surface signature of modulation of polar vortex aloft at 50 hPa. It has been documented that strength of the polar vortex is coupled with the wavelike pattern emanating from NAO at 500 hPa [29,30]. NAO modulates winter time air temperature over Eurasia which has strong inverse relationship with subsequent ISMR [20]. Thus AO has association with ISMR through modulation of NAO and Eurasian temperatures. Pre-monsoon (monthly/seasonal) AO has no significant relationship with ISMR. The concurrent relationship between AO and ISMR is strong during monsoon season and ISMR has relationship with AO in post-monsoon season.
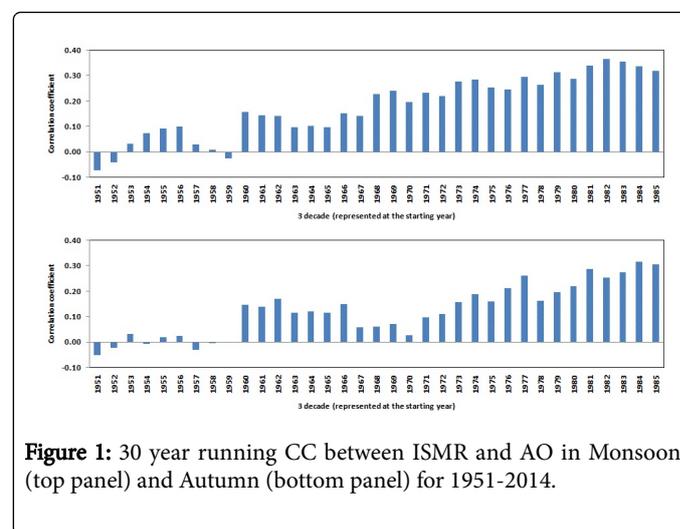

Figure 1: 30 year running CC between ISMR and AO in Monsoon (top panel) and Autumn (bottom panel) for 1951-2014.

Arctic circulation and ISMR

Shared nearest neighbor (SNN) clustering algorithm has been applied to meteorological fields in pre-monsoon months (January, February, March, April and May) and seasons (Winter and Spring) at surface, 850-hPa, 500-hPa and 200-hPa. The cluster regions which are partly or fully to the north of 50°N are referred as cluster regions in Arctic region. There are 218 cluster regions in Arctic. Cluster time series (CTSs), for 1951-2014, have been obtained for all cluster regions in Arctic by averaging corresponding meteorological field at grid points in respective cluster regions. The CCs between ISMR and these

CTSs are computed and significant CCs are found for two CTS namely (1) April 500-hPa temperature anomaly over [50°N-65°N; 95°W-130°W] (CTS1, CC=0.25) and (2) Winter 500-hPa zonal wind anomaly over [60°N-70°N; 5°W-55°W] (CTS2, CC=-0.29). Figure 2 shows 30 year sliding CCs between ISMR and CTS1 (top panel) and CTS2 (bottom panel). It is observed that the relationships between ISMR and above described CTSs are stable over time. These CTSs represents Arctic circulation conditions prior to monsoon season and hence can be used for long range forecast of ISMR. The CCs between these CTSs and monthly/seasonal AO are computed, for the period 1951-2014. The winter 500-hPa zonal wind anomaly over [60°N-70°N; 5°W-55°W] has significant positive CCs with February-AO (CC=0.29) and Winter-AO (CC=0.27). Figure 3 shows 30 year sliding CCs between CTS2 and February-AO (top panel) and Winter-AO (bottom panel). It is observed that the relationship is fluctuating in earlier stage but after 1960-90 onwards positive relationship is persisted. Thus Winter-AO is indirectly associated with ISMR by changing Winter 500-hPa zonal wind anomaly over [60°N-70°N; 5°W-55°W].
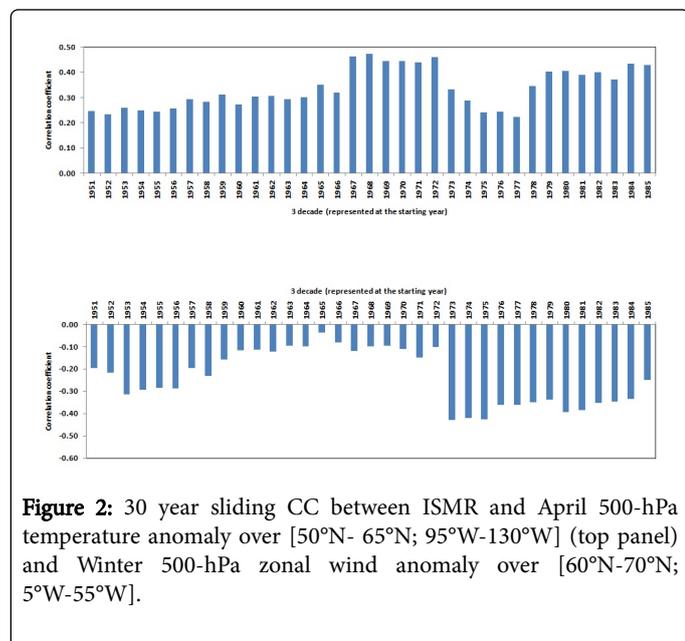

Figure 2: 30 year sliding CC between ISMR and April 500-hPa temperature anomaly over [50°N- 65°N; 95°W-130°W] (top panel) and Winter 500-hPa zonal wind anomaly over [60°N-70°N; 5°W-55°W].
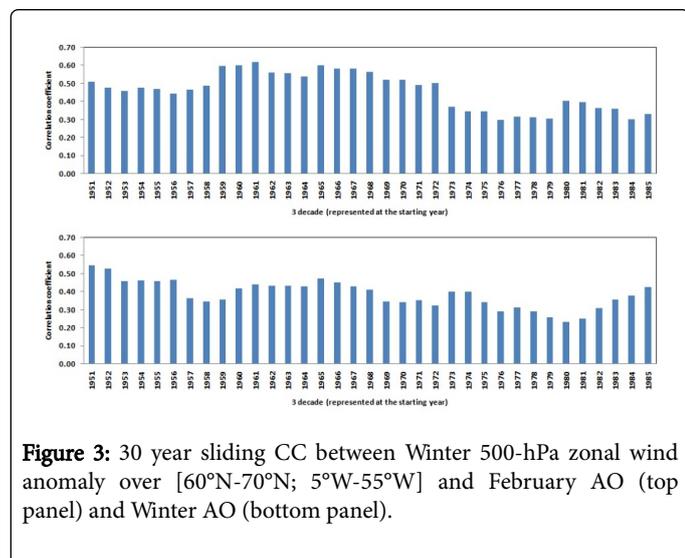

Figure 3: 30 year sliding CC between Winter 500-hPa zonal wind anomaly over [60°N-70°N; 5°W-55°W] and February AO (top panel) and Winter AO (bottom panel).

Arctic circulation and ISMR during contrasting phases of ESI-tendency

Evolution of NAO and SO from winter to spring is exactly opposite in contrasting phases of ESI-tendency. Therefore their influence on European temperature is different in two phases of ESI-tendency [10]. With this background, we have considered monthly evolution of AO pattern during contrasting phases of ESI-tendency which is important to understand the relationship of geophysical parameters over the Arctic with ISMR. The composite monthly mean AO anomaly from 1951-2014 during contrasting phases of ESI-tendency is shown in Figure 4. It reveals that AO anomaly is exactly opposite in two phases of ESI-tendency. During positive ESI-tendency, AO anomaly is negative from May to October and vice versa. Thus evolution of AO pattern, in contrasting phases of ESI-tendency, is exactly opposite.
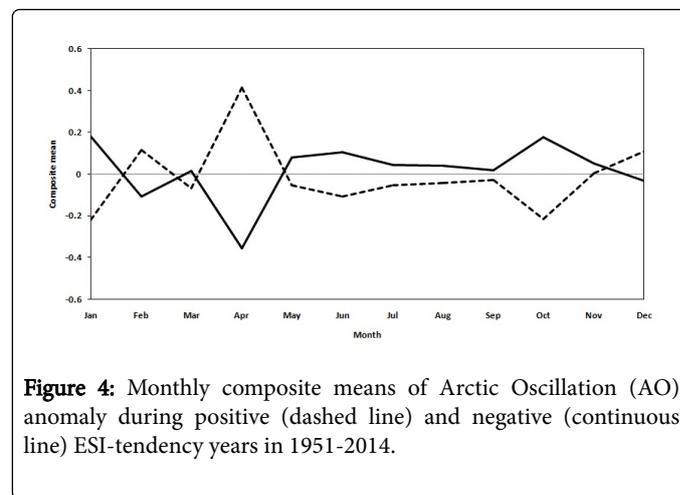

Figure 4: Monthly composite means of Arctic Oscillation (AO) anomaly during positive (dashed line) and negative (continuous line) ESI-tendency years in 1951-2014.

The relationship between predictor and ISMR drastically changes with the phase of ESI-tendency [31]. So here we have considered association of CTSs with ISMR during opposite phases of ESI-tendency. Tables 1 and 2 shows significant CC between ISMR and cluster time series during positive (CTSPs) and negative (CTSNs) ESI-tendency. During positive ESI-tendency, averaged May surface temperature anomalies over [80°N-90°N; 80E°-160°E] (CTSP1, CC=-0.38), [70°N-85°N; 5°W-20°W] (CTSP2, CC=-0.43) and [65°N-80°N; 5°E-80°E] (CTSP3, CC=-0.36) are inversely linked with ISMR. Similarly averaged May 500-hPa height anomaly over cluster region [80°N-90°N; 140°E-145°W] (CTSP4, CC=-0.39) is inversely related with ISMR. Thus, the CTSP's which significantly correlate with ISMR are in the month of May and are at surface or 500-hPa. When ESI-tendency is positive then AO anomaly is negative from May to October indicating more southward penetration of cold air mass from Arctic and hence making anomalous cooling over Eurasia. It may increase Eurasian snow-cover, which may be responsible for reduced rainfall activity over India [28,32]. During negative phase of ESI-tendency, averaged Spring 500-hPa temperature anomaly over [65°N-75°N; 0E°-25°E] (CTSN1, CC=-0.36) is inversely correlated with ISMR. Averaged May 200-hPa temperature anomalies over [25°N-55°N; 35°W-115°W] (CTSN2, CC=-0.38); [25°N-55°N; 5°W-35°W] (CTSN3, CC=-0.39) and Averaged January 200-hPa geo-potential height anomaly over [50°N-60°N; 15°W-60°W] (CTSN4, CC=-0.39) are also inversely correlated with ISMR. Thus, the CTSN's which correlate with ISMR are in pre-monsoon months/season (January, May and Spring) and at 500-hPa and 200-hPa. Thus during positive (negative) ESI-tendency, temperature, pressure conditions

over cluster regions in Arctic at surface to 500-hPa (500-hPa to 200-hPa) have relationship with ISMR. When ESI-tendency is negative then due to positive AO anomaly from May to October the southward penetration of Arctic cold air-masses is restricted, which reduces Eurasian snow-cover and hence more rainfall activity over India [28,32].

S.No.	Acronym	Location	Description	CC
1.	CTSP1	[80°N-90°N; 80E°-160°E]	Averaged May surface temperature anomaly	-0.38
2.	CTSP2	[70°N-85°N; 5°W-20°W]	Averaged May surface temperature anomaly	-0.43
3.	CTSP3	[65°N-80°N; 5°E-80°E]	Averaged May surface temperature anomaly	-0.36
4.	CTSP4	[80°N-90°N; 140°E-145°W]	Averaged May 500-hPa geo-potential height anomaly	-0.39

Table 1: Positive ESI-tendency.

S.No	Acronym	Location	Description	CC
1.	CTSN1	[65°N-75°N; 0E°-25°E]	Averaged Spring 500-hPa temperature anomaly	-0.36
2.	CTSN2	[25°N-55°N; 35°W-115°W]	Averaged May 200-hPa temperature anomaly	-0.38
3.	CTSN3	[25°N-55°N; 5°W-35°W]	Averaged May 200-hPa temperature anomaly	-0.39
4.	CTSN4	[50°N-60°N; 15°W-60°W]	Averaged January 200-hPa geo-potential height anomaly	-0.39

Table 2: Negative ESI-tendency.

Conclusions

From the above analysis, following conclusions can be drawn:

AO and ISMR show direct concurrent relationship with each other in monsoon season. Winter-AO is indirectly related with ISMR through its influence on mid-tropospheric zonal wind anomaly over [60°N-70°N; 5°W-55°W] [33].

In both the phases of ESI-tendency, there is statistically significant inverse relationship between cluster time series in Arctic region and ISMR.

The significant relationship between cluster time series in Arctic region and ISMR show spatial and temporal variability in positive and negative ESI-tendency [34].

During positive (negative) ESI-tendency, lower tropospheric (upper tropospheric) temperature, pressure anomalies over respective cluster regions in Arctic affects ISMR.

Due to the statistically significant relationship between the circulation over Arctic in pre-monsoon months and ISMR, the circulation parameters over Arctic can be good predictors for ISMR.

Acknowledgement

References

1. Thompson DW, Wallace JM (1998) The Arctic Oscillation signature in the wintertime geopotential height and temperature fields. Geophys Res Lett 25: 1297-1300.
2. Wu A, Hsieh WW, Shabbar A, Boer GJ, Zwiers FW (2006) The nonlinear association between the Arctic Oscillation and North American winter climate. Clim Dynam 26: 865-879.
3. Huang W, Wang B, Wright JS, Chen R (2016) On the non-stationary relationship between the Siberian high and Arctic oscillation. PloS one 11: e0158122.
4. Huang W, Wang B, Wright JS (2016) A potential vorticity based index for the East Asian winter monsoon. J Geophy Res: Atmos 121: 9382-9399.
5. Park TW, Ho CH, Yang S (2011) Relationship between the Arctic Oscillation and cold surges over East Asia. J Clim 24: 68-83.
6. Gong DY, Wang SW, Zhu JH (2001) East Asian Winter Monsoon and Arctic Oscillation. Geophys Res Lett 28: 2073-2076.
7. Kakade SB, Dugam SS (2000) Simultaneous effect of NAO and SO on the monsoon activity over India. Geophys Res Lett 27:3501-3504.
8. Kakade SB, Dugam SS (2006) Spatial monsoon variability with respect to NAO and SO. J Earth Syst Sci 115: 601-606.
9. Kakade SB, Dugam SS (2006) North Atlantic Oscillation and northern hemispheric warming. Indian J Mar Sci 35:205-209.
10. Kakade SB, Kulkarni A (2011) Relationship between ESI tendency and Indian monsoon rainfall: a possible mechanism. Atmos Sci Let 13: 22-28.
11. Kakade SB, Kulkarni A (2012) The changing relationship between surface temperatures and Indian monsoon rainfall with the phase of ESI tendency. Adv in Meteorol pp: 1-8.

12. Scaife AA, Folland CK, Alexander LV, Moberg A, Knight JR (2008) European climate extremes and the North Atlantic Oscillation. J Climate 21: 72-83.

13. Lund IA (1963) Map-pattern classification by statistical methods. J Appl Meteorol 2: 56-65.

14. Kulkarni A, Kripalani RH, Singh SV (1992) Classification of summer monsoon rainfall patterns over India. Int J Climatol 12: 269-280.

15. Kruizinga S (1979) Objective classification of daily 500 mb patterns. Sixth Conference on Probability and Statistics in Atmospheric Sciences, Am Met Soc Bostoon, Masachettus: 126-129.

16. Mo K, Ghil M (1988) Cluster analysis of multiple planetary flow regimes. J Geophy Res: Atmos 93: 10927-10952.

17. Michelangeli PA, Vautard R, Legras B (1995) Weather regimes: Recurrence and quasi stationarity. J Atmos Sci 52: 1237-1256.

18. Robertson AW, Ghil M (1999) Large-scale weather regimes and local climate over the western United States. J Climate 12: 1796-1813.

19. Zadeh LA (1965) Fuzzy sets. Inf Contr 8: 338-353.

20. Kulkarni A, Kripalani RH (1998) Rainfall patterns over India: Classification with Fuzzy-c means method. Theor Appld Climatol 59: 137-146.

21. Huang W, Chen R, Wang B, Wright JS, Yang Z, et al. (2017) Potential vorticity regimes over East Asia during winter. J Geophy Res: Atmos 122: 1524-1544.

22. Chen R, Huang W, Wang B, Yang Z, Wright JS, et al. (2017) On the co-occurrence of wintertime temperature anomalies over eastern Asia and eastern North America. J Geophy Res: Atmos 122: 6435.

23. Caraway NM, McCreight JL, Rajagopalan B (2014) Multisite stochastic weather generation using cluster analysis and k-nearest neighbor time series resampling. J Hydrol 508: 197-213.

24. Ertoz L, Steinbach M, Kumar V (2003) Finding clusters of different sizes, shapes, and densities in noisy, high dimensional data. Proceedings of Third SIAM International Conference on Data Mining, San Francisco, CA, USA.

25. Steinbach M, Klooster S, Potter C, Kumar V (2003) Discovery of climate indices using clustering. KDD, Washington, DC, USA.

26. Boriah S, Simon G, Naorem M, Steinbach M, Kumar V, et al. (2004) Predicting Land Temperature Using Ocean Data. KDD Seattle, WA, USA.

27. Jarvis RA, Patrick EA (1973) Clustering using a similarity measure based on shared nearest neighbors. IEEE Trans Comput C-22: 1025-1034.

28. Bamzai A, Shukla J (1999) Relation between Eursian snow cover, snow depth, and the Indian summer monsoon: An observational study. J Climate 12: 3117-3132.

29. Baldwin MP, Cheng X, Dunkerton TJ (1994) Observed correlationsbetween winter-mean tropospheric and stratospheric circulation anomalies. Geophys Re. Lett 21: 1141-1144.

30. Perlwitz J, Graf HF (1995) The statistical connection between tropospheric and stratospheric circulation of the Northern Hemisphere in winter. J Climate 8: 2281-2295.

31. Kakade SB, Kulkarni A (2016) Prediction of summer monsoon rainfall over India and its homogeneous regions. Meteorol Appl 1: 1-13.

32. Kriapalni RH, Kulkarni A (1999) Climatology and variability of historical Soviet snow depth data: some new perspectives in snow-Indian monsoon teleconnections. Clim Dynam 15: 475-489.

33. Maykut GA (1978) Energy Exchange over young sea-ice in the central Arctic. J Geophy Res: Atmos 83: 3646-3658.

34. Prabhu A, Mahajan PN, Khaladkar RM (2012) Association of the Indian summer monsoon rainfall variability with the geophysical parameters over the Arctic region. Int J Climatol 32: 2042-2050.